X-Ray Crystal Structures and Unusual Magnetic Properties of Alkoxo-Bridged Copper(II) Complexes with 2-Dialkylaminoethanol and 1-Dialkylamino-2-propanol

Masahiro MIKURIYA,* Masato YAMAMOTO, and Wasuke MORI†,#
Department of Chemistry, School of Science, Kwansei Gakuin University, Uegahara, Nishinomiya 662
† Institute of Chemistry, College of General Education, Osaka University, Toyonaka, Osaka 560
(Received January 7, 1994)

A series of alkoxo-bridged copper(II) complexes with 2-dialkylaminoethanol and 1-dialkylamino-2-propanol, $[Cu_2(R_2NCH_2CH_2O)_2(NCS)_2]$ and $[Cu_2\{R_2NCH_2CH(CH_3)O\}_2(NCS)_2]$ (R=CH_3, C_2H_5, n-C_3H_7, i-C_3H_7), have been prepared and characterized by infrared and electronic spectroscopies, and temperature dependence of magnetic susceptibilities. The crystal structures of $[Cu_2\{i\text{-}C_3H_7)_2NCH_2CH_2O\}_2(NCS)_2]$ and $[Cu_2\{R_2NCH_2CH(CH_3)O\}_2(NCS)_2]$ (R=CH_3, C_2H_5, n-C_3H_7, i-C_3H_7) have been determined by X-ray crystallography. The compounds are polymeric with copper atoms alternately bridged by two alkoxo oxygen atoms and two thiocyanate ions, except for $[Cu_2\{(i\text{-}C_3H_7)_2NCH_2CH(CH_3)O\}_2(NCS)_2]$ which is a discrete alkoxo-bridged dinuclear molecule. The unusual magnetic properties are discussed in relation to the crystal structures.

For many years, a great number of dinuclear copper(II) complexes have been prepared, and their crystal structures and magnetic properties have been extensively studied in order to elucidate the correlation between them. As a result of these studies, significant progress has been made in the understanding of the spin-exchange interaction phenomenon.[1—5] In most of these dinuclear copper(II) complexes reported so far, the experimental behavior of the magnetic susceptibilities has been well explained by the so-called Bleaney–Bowers formula based on the Heisenberg model.[6] However, in a few cases, the Bleaney–Bowers formula is unable to explain the magnetic behavior of the dinuclear copper(II) system.[7—12] In 1971, Lehtonen et al. found that the temperature dependence of the magnetic susceptibility (90—300 K) of an alkoxo-bridged copper(II) complex with 2-diethylaminoethanol, $[Cu_2\{(C_2H_5)_2NCH_2CH_2O\}_2(NCS)_2]$, could not be interpreted by the Bleaney–Bowers equation and assumed that this compound did not have a simple dinuclear structure.[13] The X-ray crystal structure was subsequently determined by Pajunen et al. in 1974.[14] The structure essentially consists of alkoxo-bridged dinuclear units. However, the dinuclear units are weakly linked through thiocyanate bridges [Cu···S distance 2.851(4) Å, Cu···Cu (interdimer) distance 5.653(2) Å]. Thus, the crystal structure can be viewed as an alternating chain structure. Later, Haase, Nishida, Kida, et al. studied the crystal structures of this type of compounds together with their magnetic properties in the temperature range 80—300 K, and found that two compounds, $[Cu_2\{(CH_3)_2NCH_2CH_2O\}_2(NCS)_2]$ and $[Cu_2\{(n\text{-}C_3H_7)_2NCH_2CH_2O\}_2(NCS)_2]$, have a similar alternating chain structure [Cu···S distance 2.846(6)—3.073(2) Å, Cu···Cu (interdimer) distance 5.362—5.727(2) Å.][15—17] They could not interpret the susceptibility data of these compounds by the Bleaney–Bowers equation and, thus, they attributed this unusual magnetic behavior to an interdimer interaction through the thiocyanate bridges. However, judging from the interdimer contacts, it would seem unlikely that such an interdimer interaction is strong enough to cause the observed large deviation of the susceptibility data from the dimer model. Hence further experimental work is necessary to explain this result. First, it is desirable to extend susceptibility measurements down to the liquid-helium temperature. Second, it is important to collect more examples of similar dialkoxo-bridged copper(II) complexes which show the above-mentioned unusual magnetic properties. Up to now, the X-ray structural studies have been limited to only three compounds, $[Cu_2(R_2NCH_2CH_2O)_2(NCS)_2]$ (R=CH_3, C_2H_5, n-C_3H_7).[14,15,17] In this work, we have synthesized more examples of this type of compounds by using 2-diisopropylaminoethanol, 1-dipropylamino-2-propanol, and 1-diisopropylamino-2-propanol. Furthermore, we have prepared the previously reported ones, $[Cu_2(R_2NCH_2CH_2O)_2(NCS)_2]$ and $[Cu_2\{R_2NCH_2CH(CH_3)O\}_2(NCS)_2]$, but we have used the abbreviations $[Cu_2(R\text{-}L)_2(NCS)_2]$ and $[Cu_2(R\text{-}L')_2(NCS)_2]$, respectively, where R=$CH_3$, C_2H_5, n-C_3H_7, i-C_3H_7 (Chart 1). Measurements of the magnetic properties have been carried out down to 4 K.

Experimental

Ligand Synthesis. 2-Dialkylaminoethanol and 1-di-

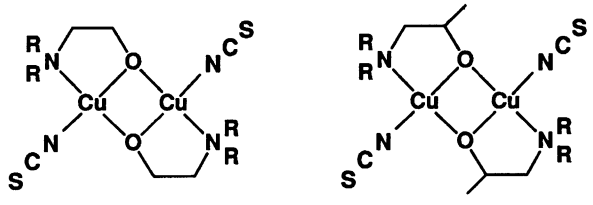

$[Cu_2(R\text{-}L)_2(NCS)_2]$ $[Cu_2(R\text{-}L')_2(NCS)_2]$

Chart 1.

#Present address: Department of Chemistry, Faculty of Science, Osaka University, Toyonaka, Osaka 560.

alkylamino-2-propanol (abbreviated as HR-L and HR-L′, respectively) were prepared by applying methods described in the literatures.[18,19]

Preparation of Complexes. **$[Cu_2(CH_3\text{-}L)_2(NCS)_2]$.** This compound was prepared as described by Nishida and Kida.[16] Slow evaporation of the methanol solution resulted in bluish green crystals suitable for X-ray analysis and magnetic measurement. Anal. Calcd for $C_5H_{10}CuN_2OS$: C, 28.63; H, 4.81; N, 13.36%. Found: C, 28.62; H, 5.02; N, 13.43%. IR (Nujol mull) ν/cm^{-1} ν(NCS) 2112. Electronic spectrum in $CHCl_3$ λ_{max}/nm (ε per $Cu/dm^3\,mol^{-1}\,cm^{-1}$) 642 (177), 377 (2140). Diffuse reflectance spectrum λ_{max}/nm 655, 375. μ_{eff} (297 K)/B.M. 1.26.

$[Cu_2(C_2H_5\text{-}L)_2(NCS)_2]$. This compound was prepared by a procedure analogous to that described by Lehtonen et al.[13] Anal. Calcd for $C_7H_{14}CuN_2OS$: C, 35.36; H, 6.93; N, 11.78%. Found: C, 35.58; H, 5.18; N, 11.80%. IR (Nujol mull) ν/cm^{-1} ν(NCS) 2112. Electronic spectrum in $CHCl_3$ λ_{max}/nm (ε per $Cu/dm^3\,mol^{-1}\,cm^{-1}$) 658 (182), 384 (2240). Diffuse reflectance spectrum λ_{max}/nm 687, 375. μ_{eff} (297 K)/B.M. 1.32.

$[Cu_2(n\text{-}C_3H_7\text{-}L)_2(NCS)_2]$. This compound was prepared by the procedure described by Nishida and Kida.[16] Anal. Calcd for $C_9H_{18}CuN_2OS$: C, 40.66; H, 6.82; N, 10.54%. Found: C, 40.60; H, 7.05; N, 10.66%. IR (Nujol mull) ν/cm^{-1} ν(NCS) 2108. Electronic spectrum in $CHCl_3$ λ_{max}/nm (ε per $Cu/dm^3\,mol^{-1}\,cm^{-1}$) 653 (188), 385 (2480). Diffuse reflectance spectrum λ_{max}/nm 697, 375. μ_{eff} (317 K)/B.M. 1.36.

$[Cu_2(i\text{-}C_3H_7\text{-}L)_2(NCS)_2]$. To a methanol solution (15 ml) of 2-diisopropylaminoethanol (223 mg, 1.54 mmol) and copper(II) acetate monohydrate (100 mg, 0.501 mmol), a methanol solution (20 ml) of ammonium thiocyanate (38 mg, 0.50 mmol) was added. The reaction mixture was allowed to stand at 5 °C for several days. Bluish green crystals separated, and were collected by filtration and then dried in vacuo over P_2O_5. Yield: 11 mg (8%). Anal. Calcd for $C_9H_{18}CuN_2OS$: C, 40.66; H, 6.82; N, 10.54%. Found: C, 40.33; H, 6.99; N, 10.56%. IR (Nujol mull) $\nu/cm^{-1}\nu$(NCS) 2108. Electronic spectrum in $CHCl_3$ λ_{max}/nm (ε per $Cu/dm^3\,mol^{-1}\,cm^{-1}$) 647 (162), 386 (1690). Diffuse reflectance spectrum λ_{max}/nm 691, 370. μ_{eff} (317 K)/B.M. 1.35.

$[Cu_2(CH_3\text{-}L')_2(NCS)_2]$. This compound was prepared by the procedure described by Nishida and Kida.[16] Anal. Calcd for $C_6H_{12}CuN_2OS$: C, 32.20; H, 5.40; N, 12.52%. Found: C, 32.12; H, 5.52; N, 12.47%. IR (Nujol mull) ν/cm^{-1} ν(NCS) 2104. Electronic spectrum in $CHCl_3$ λ_{max}/nm (ε per $Cu/dm^3\,mol^{-1}\,cm^{-1}$) 640 (177), 377 (1810). Diffuse reflectance spectrum λ_{max}/nm 680, 370. μ_{eff} (317 K)/B.M. 1.29.

$[Cu_2(C_2H_5\text{-}L')_2(NCS)_2]$. This compound was prepared by a procedure similar to that described by Nishida and Kida.[16] Anal. Calcd for $C_8H_{16}CuN_2OS$: C, 37.93; H, 6.38; N, 11.07%. Found: C, 38.16; H, 6.40; N, 11.12%. IR (Nujol mull) ν/cm^{-1} ν(NCS) 2112. Electronic spectrum in $CHCl_3$ λ_{max}/nm (ε per $Cu/dm^3\,mol^{-1}\,cm^{-1}$) 645 (172), 386 (1820). Diffuse reflectance spectrum λ_{max}/nm 701, 370. μ_{eff} (300 K)/B.M. 1.54.

$[Cu_2(n\text{-}C_3H_7\text{-}L')_2(NCS)_2]$. Triethylamine (202 mg, 2.00 mmol) and ammonium thiocyanate (38 mg, 0.50 mmol) were successively added to a solution containing copper(II) acetate monohydrate (100 mg, 0.501 mmol) and 1-dipropylamino-2-propanol (160 mg, 1.00 mmol) in 40 ml of methanol. Bluish green crystals were obtained on standing at 5 °C for several days. They were collected by filtration, washed with methanol, and dried in vacuo over P_2O_5. Yield: 22 mg (16%). Anal. Calcd for $C_{10}H_{20}CuN_2OS$: C, 42.91; H, 7.20; N, 10.01%. Found: C, 42.94; H, 7.28; N, 10.15%. IR (Nujol mull) ν/cm^{-1} ν(NCS) 2096. Electronic spectrum in $CHCl_3$ λ_{max}/nm (ε per $Cu/dm^3\,mol^{-1}\,cm^{-1}$) 646 (165), 388 (2090). Diffuse reflectance spectrum λ_{max}/nm 706, 375. μ_{eff} (317 K)/B.M. 1.32.

$[Cu_2(i\text{-}C_3H_7\text{-}L')_2(NCS)_2]$. 1-Diisopropylamino-2-propanol (160 mg, 1.00 mmol) was added to a solution of copper(II) acetate monohydrate (100 mg, 0.501 mmol) in methanol (5 ml). Then triethylamine (101 mg, 1.00 mmol) and ammonium thiocyanate (38 mg, 0.50 mmol) were successively added. The bluish green crystals which formed were collected by filtration, washed with methanol, and dried in vacuo over P_2O_5. Yield: 14 mg (10%). Anal. Calcd for $C_{10}H_{20}CuN_2OS$: C, 42.91; H, 7.20; N, 10.01%. Found: C, 42.85; H, 7.38; N, 9.87%. IR (Nujol mull) ν/cm^{-1} ν(NCS) 2080. Electronic spectrum in $CHCl_3$ λ_{max}/nm (ε per $Cu/dm^3\,mol^{-1}\,cm^{-1}$) 654 (159), 380 (1270). Diffuse reflectance spectrum λ_{max}/nm 667, 370. μ_{eff} (317 K)/B.M. 1.56.

Measurements. A Perkin–Elmer 2400 Series II CHNS/O Analyzer was used to collect microanalytical data (C, H, N). Infrared spectra were measured on a Hitachi 270-30 Infrared Spectrophotometer in the 4000—400 cm^{-1} region on a Nujol mull. Electronic spectra were measured using a Shimadzu UV-vis-NIR Recording Spectrophotometer (Model UV-3100). Magnetic susceptibilities were measured by the Faraday method over the temperature range 8—317 K. The susceptibilitis were corrected for the diamagnetism of the constituent atoms using Pascal's constants.[20] The effective magnetic moments were calculated from the equation $\mu_{eff}=2.828\sqrt{\chi_A T}$, where χ_A is the atomic magnetic susceptibility.

X-Ray Crystal Structure Analysis. Diffraction data were collected on an Enraf–Nonius CAD4 diffractometer using graphite-monochromated Mo $K\alpha$ radiation at 25±1 °C. Crystal data and details concerning data collection are given in Table 1. The lattice constants were determined by a least-squares refinement based on 25 reflections with $20\leq 2\theta\leq 30°$. The intensity data were corrected for Lorentz-polarization effects, but not for absorption. The structures were solved by direct methods. Refinements were carried out by the full-matrix least-squares methods. Hydrogen atoms were located from difference Fourier maps and fixed at their positions. The weighting scheme, $w=1/[\sigma^2(|F_o|)+(0.02|F_o|)^2+1.0]$, was employed. The final discrepancy factors, $R=\sum||F_o|-|F_c||/\sum|F_o|$ and $R_w=[\sum w(|F_o|-|F_c|)^2/\sum w|F_o|^2]^{1/2}$, are listed in Table 1. All of the calculations were carried out on a Micro-VAXII computer using an Enraf–Nonius SDP program package.[21] The atomic coordinates and thermal parameters of the non-hydrogen atoms are listed in Table 2. The anisotropic thermal parameters of the non-hydrogen atoms, the atomic coordinates and temperature factors of the hydrogen atoms, and the F_o-F_c tables were deposited as Document No. 67032 at the Office of the Editor of Bull. Chem. Soc. Jpn.

Table 1. Crystal Data and Data Collection Details

Complexes	$[Cu_2(i\text{-}C_3H_7\text{-}L)_2(NCS)_2]$	$[Cu_2(CH_3\text{-}L')_2(NCS)_2]$	$[Cu_2(C_2H_5\text{-}L')_2(NCS)_2]$
Formula	$Cu_2S_2O_2N_4C_{18}H_{36}$	$Cu_2S_2O_2N_4C_{12}H_{24}$	$Cu_2S_2O_2N_4C_{16}H_{32}$
F.W.	531.7	447.6	503.7
Crystal system	Triclinic	Triclinic	Monoclinic
Space group	$P\bar{1}$	$P\bar{1}$	$P2_1/c$
a/Å	7.876(2)	8.120(5)	8.041(14)
b/Å	10.245(3)	8.461(2)	15.129(6)
c/Å	7.748(3)	6.998(2)	9.531(12)
α/°	102.77(3)	93.92(3)	
β/°	93.80(2)	105.00(4)	103.45(6)
γ/°	84.25(2)	96.65(4)	
V/Å^3	606.0(3)	458.8(4)	1127.7(24)
Z	1	1	2
D_c/g cm^{-3}	1.46	1.62	1.49
D_m/g cm^{-3}	1.46	1.62	1.44
$F(000)$	278	230	524
μ(Mo $K\alpha$)/cm^{-1}	19.45	25.53	20.31
Crystal dimensions (mm)	0.07×0.18×0.32	0.13×0.20×0.32	0.12×0.25×0.31
2θ range/°	2.0—50.0	2.0—50.0	2.0—50.0
Total no. of observed reflections	2114	1607	2074
No. of unique reflections with $I>3\sigma(I)$	1403	1316	1062
Final no. of variables	127	100	118
Final rediduals			
R	0.052	0.044	0.056
R_w	0.058	0.067	0.063

Complexes	$[Cu_2(n\text{-}C_3H_7\text{-}L')_2(NCS)_2]$	$[Cu_2(i\text{-}C_3H_7\text{-}L')_2(NCS)_2]$
Formula	$Cu_2S_2O_2N_4C_{20}H_{40}$	$Cu_2S_2O_2N_4C_{20}H_{40}$
F.W.	559.8	559.8
Crystal system	Monoclinic	Monoclinic
Space group	$P2_1/n$	$P2_1/n$
a/Å	11.627(4)	11.223(8)
b/Å	14.176(5)	14.598(5)
c/Å	8.175(3)	8.159(6)
α/°		
β/°	95.72(2)	92.49(3)
γ/°		
V/Å^3	1340.8(8)	1335.4(14)
Z	2	2
D_c/g cm^{-3}	1.39	1.39
D_m/g cm^{-3}	1.39	1.39
$F(000)$	588	588
μ(Mo $K\alpha$)/cm^{-1}	17.69	17.62
Crystal dimensions (mm)	0.07×0.33×0.42	0.12×0.31×0.55
2θ range/°	2.0—50.0	2.0—50.0
Total no. of observed reflections	2467	2449
No. of unique reflections with $I>3\sigma(I)$	1339	1616
Final no. of variables	134	136
Final rediduals		
R	0.057	0.048
R_w	0.061	0.057

Results and Discussion

Description of the Crystal Structures. $[Cu_2(i\text{-}C_3H_7\text{-}L)_2(NCS)_2]$. The molecular structure of $[Cu_2(i\text{-}C_3H_7\text{-}L)_2(NCS)_2]$ is substantially similar to those of the methyl, ethyl, *n*-propyl derivatives already reported: $[Cu_2(CH_3\text{-}L)_2(NCS)_2]$,[15] $[Cu_2(C_2H_5\text{-}L)_2(NCS)_2]$,[14] and $[Cu_2(n\text{-}C_3H_7\text{-}L)_2(NCS)_2]$.[17] A per-

Table 2. Fractional Positional Parameters and Thermal Parameters of Non-Hydrogen Atoms with Their Estimated Standard Deviations in Parentheses

Atom	x	y	z	B_{eq}/Å^{2} a)
$[Cu_2(i\text{-}C_3H_7\text{-}L)_2(NCS)_2]$				
Cu	0.5556(1)	0.4111(1)	0.8311(1)	3.75(2)
S	0.3167(3)	0.3433(2)	0.2534(3)	5.44(5)
O	0.6447(6)	0.4811(5)	1.0633(6)	3.7(1)
N1	0.7506(8)	0.2564(6)	0.8325(7)	3.9(1)
N2	0.4559(9)	0.3618(7)	0.5953(8)	4.8(2)
C1	0.774(1)	0.4019(9)	1.131(1)	5.1(2)
C2	0.769(1)	0.257(1)	1.024(1)	6.7(3)
C3	0.901(1)	0.303(1)	0.765(1)	6.2(2)
C4	0.891(1)	0.301(1)	0.570(1)	6.9(3)
C5	1.078(1)	0.241(1)	0.816(2)	7.9(3)
C6	0.696(1)	0.1210(9)	0.727(1)	7.0(3)
C7	0.528(1)	0.092(1)	0.772(2)	7.1(3)
C8	0.826(2)	0.001(1)	0.735(2)	12.6(5)
C9	0.3973(9)	0.3542(7)	0.4536(9)	3.5(2)
$[Cu_2(CH_3\text{-}L')_2(NCS)_2]$				
Cu	0.6785(1)	0.5737(1)	0.0087(1)	2.43(2)
S	1.1503(2)	0.6310(3)	−0.2559(3)	3.43(4)
O	0.5087(6)	0.5839(7)	0.1531(8)	2.9(1)
N1	0.7793(8)	0.7957(8)	0.156(1)	3.2(2)
N2	0.8386(8)	0.5838(9)	−0.153(1)	3.2(1)
C1	0.513(1)	0.733(1)	0.257(1)	3.6(2)
C2	0.697(1)	0.808(1)	0.325(1)	3.8(2)
C3	0.439(1)	0.720(1)	0.435(1)	4.6(2)
C4	0.970(1)	0.826(1)	0.239(2)	4.6(2)
C5	0.722(1)	0.911(1)	0.018(2)	5.1(3)
C6	0.969(1)	0.605(1)	−0.200(1)	2.6(2)
$[Cu_2(C_2H_5\text{-}L')_2(NCS)_2]$				
Cu	0.1767(1)	0.52044(9)	0.5825(1)	3.47(2)
S	0.7412(3)	0.4159(2)	0.6853(3)	4.68(7)
O	−0.0385(7)	0.5783(4)	0.5148(7)	3.7(2)
N1	0.2081(9)	0.6117(6)	0.7473(8)	3.8(2)
N2	0.4001(9)	0.4654(6)	0.6343(8)	4.1(2)
C1	−0.079(1)	0.6488(7)	0.595(1)	4.1(2)
C2	0.090(1)	0.6846(7)	0.684(1)	4.4(3)
C3	−0.178(1)	0.7217(8)	0.504(1)	6.0(3)
C4	0.142(1)	0.5693(9)	0.866(1)	5.9(3)
C5	0.221(2)	0.482(1)	0.918(1)	6.9(3)
C6	0.385(1)	0.6465(9)	0.807(1)	6.3(3)
C7	0.468(1)	0.6873(9)	0.695(1)	6.3(3)
C8	0.542(1)	0.4452(7)	0.658(1)	3.4(2)
Atom	x	y	z	B_{eq}/Å^{2} a)
$[Cu_2(n\text{-}C_3H_7\text{-}L')_2(NCS)_2]$				
Cu	0.0687(1)	0.49189(8)	0.1634(1)	6.11(2)
S	0.0826(3)	0.3653(2)	0.6856(3)	6.68(6)
O	0.0495(5)	0.5761(4)	−0.0193(6)	6.0(1)
N1	0.2350(7)	0.5461(5)	0.1834(8)	6.3(2)
N2	0.0744(8)	0.4167(6)	0.3597(8)	7.4(2)
C1	0.1358(9)	0.6429(7)	−0.042(1)	6.6(2)
C2	0.219(1)	0.6447(7)	0.115(1)	7.5(3)
C3	0.081(1)	0.7402(7)	−0.076(1)	8.9(3)
C4	0.3048(9)	0.4919(8)	0.075(1)	7.3(3)
C5	0.310(1)	0.3879(7)	0.105(1)	8.2(3)
C6	0.380(1)	0.3390(8)	−0.013(2)	9.1(3)
C7a	0.248(2)	0.551(2)	0.383(3)	5.4(5)*
C7b	0.326(1)	0.547(1)	0.342(2)	5.1(3)*
C8a	0.352(2)	0.609(2)	0.425(3)	6.3(5)*
C8b	0.276(1)	0.612(1)	0.473(2)	6.0(3)*
C9	0.361(1)	0.5927(9)	0.630(1)	8.8(3)
C10	0.0786(8)	0.3954(6)	0.4948(9)	5.3(2)
$[Cu_2(i\text{-}C_3H_7\text{-}L')_2(NCS)_2]$				
Cu	0.45471(7)	0.08373(5)	0.9131(1)	3.46(1)
S	0.5216(2)	0.3875(1)	0.8161(3)	5.89(5)
O	0.3975(4)	−0.0185(3)	1.0265(6)	4.7(1)
N1	0.2861(4)	0.1032(3)	0.8237(6)	3.1(1)
N2	0.5242(5)	0.2000(4)	0.8582(8)	5.2(1)
C1	0.2812(6)	−0.0447(5)	0.988(1)	5.4(2)
C2	0.2109(5)	0.0352(4)	0.9159(8)	3.6(1)
C3	0.2187(7)	−0.0876(5)	1.1256(9)	5.5(2)
C4	0.2427(6)	0.1997(4)	0.8584(8)	4.1(1)
C5	0.2686(7)	0.2257(5)	1.0388(9)	5.4(2)
C6	0.1112(7)	0.2154(5)	0.805(1)	6.1(2)
C7	0.2773(6)	0.0814(5)	0.6408(8)	4.4(1)
C8	0.3350(9)	0.1541(6)	0.536(1)	7.1(2)
C9	0.333(1)	−0.0118(6)	0.608(1)	7.2(2)
C10	0.5239(5)	0.2780(5)	0.8406(8)	4.2(1)

a) Anisotropically refined atoms are given in the form of the isotropic equivalent thermal parameter defined as $4/3[a^2B(1,1)+b^2B(2,2)+c^2B(3,3)+ab(\cos\gamma)B(1,2)+ac(\cos\beta)B(1,3)+bc(\cos\alpha)B(2,3)]$. Starred atoms were refined isotropically.

spective drawing of the molecule is illustrated in Fig. 1. Selected bond distances and angles are listed in Table 3. The crystal structure essentially consists of dialkoxo-bridged dinuclear units, $[Cu_2(i\text{-}C_3H_7\text{-}L)_2(NCS)_2]$, which are located at the crystallographic inversion center. The Cu···Cu′ distance is 2.968(1) Å and the Cu–O–Cu′ angle is 100.9(3)°. Each copper atom is coordinated to two alkoxo-oxygen atoms, an amino nitrogen atom, and a thiocyanate nitrogen atom in the square plane. The Cu–O, Cu–O′, Cu–N1, and Cu–N2 bond distances are 1.899(4), 1.949(5), 2.095(6), and 1.922(6) Å, respectively, and are typical for coordination bonds of dialkoxo-bridged dinuclear copper(II) complexes.[22—25] In addition, a thiocyanate S atom of a neighboring dinuclear unit approaches the copper atom with a Cu···S distance of 3.015(3) Å. The coordination sphere around the copper atom can be considered as a distorted square-pyramidal (4+1) stereochemistry if the long Cu···S distance is taken into account, and the thiocyanate groups form bridges between the dinuclear units. Thus, a one-dimensional chain is formed by alternating dialkoxo-bridged Cu$\langle_{O}^{O}\rangle$Cu units and dithiocyanato-bridged Cu$\langle_{SCN}^{NCS}$Cu units (Fig. 2). The interdimer Cu···Cu separation is 5.798(1) Å.

Table 3. Selected Interatomic Distances (l/Å) and Bond Angles (ϕ/°) with Their Estimated Standard Deviations in Parentheses

Complex	$[Cu_2(i\text{-}C_3H_7\text{-}L)_2(NCS)_2]$	$[Cu_2(CH_3\text{-}L')_2(NCS)_2]$	$[Cu_2(C_2H_5\text{-}L')_2(NCS)_2]$	$[Cu_2(n\text{-}C_3H_7\text{-}L')_2(NCS)_2]$	$[Cu_2(i\text{-}C_3H_7\text{-}L')_2(NCS)_2]$
Cu···Cu′ a)	2.968(1)	2.988(1)	2.975(1)	2.981(1)	2.963(1)
Cu–O	1.899(4)	1.914(6)	1.912(6)	1.907(5)	1.894(4)
Cu–O′	1.949(5)	1.950(5)	1.961(6)	1.970(6)	1.931(4)
Cu–N1	2.095(6)	2.050(7)	2.061(8)	2.072(8)	2.047(5)
Cu–N2	1.922(6)	1.931(8)	1.937(7)	1.923(7)	1.916(6)
Cu···S″ b)	3.015(3)	2.765(2)	2.943(3)	3.025(3)	
Cu···Cu″	5.798(1)	5.537(1)	5.805(2)	5.887(1)	
O–Cu–O′	79.1(2)	78.7(2)	79.6(3)	79.5(2)	78.5(2)
O–Cu–N1	84.2(2)	84.4(3)	83.8(3)	82.3(2)	86.3(2)
O′–Cu–N2	96.6(2)	101.5(2)	100.5(3)	101.1(3)	99.4(2)
N1–Cu–N2	101.9(2)	92.9(3)	98.7(3)	100.7(3)	99.4(2)
Cu–O–Cu′	100.9(3)	101.3(3)	100.4(3)	100.5(3)	101.5(2)
Cu–O–C1	116.8(3)	115.4(5)	118.3(5)	119.7(5)	117.3(4)
Cu′–O–C1	132.2(4)	133.1(5)	131.4(5)	135.7(4)	134.3(4)

a) Prime refers to the equivalent positions $(1-x, 1-y, 2-z)$, $(1-x, 1-y, -z)$, $(-x, 1-y, 1-z)$, $(-x, 1-y, -z)$, and $(1-x, -y, 2-z)$ for $[Cu_2(i\text{-}C_3H_7\text{-}L)_2(NCS)_2]$, $[Cu_2(CH_3\text{-}L')_2(NCS)_2]$, $[Cu_2(C_2H_5\text{-}L')_2(NCS)_2]$, $[Cu_2(n\text{-}C_3H_7\text{-}L')_2(NCS)_2]$, and $[Cu_2(i\text{-}C_3H_7\text{-}L')_2(NCS)_2]$, respectively. b) Double prime refers to the equivalent positions $(1-x, 1-y, 1-z)$, $(2-x, 1-y, -z)$, $(1-x, 1-y, 1-z)$, and $(-x, 1-y, 1-z)$ for $[Cu_2(i\text{-}C_3H_7\text{-}L)_2(NCS)_2]$, $[Cu_2(CH_3\text{-}L')_2(NCS)_2]$, $[Cu_2(C_2H_5\text{-}L')_2(NCS)_2]$, and $[Cu_2(n\text{-}C_3H_7\text{-}L')_2(NCS)_2]$, respectively.

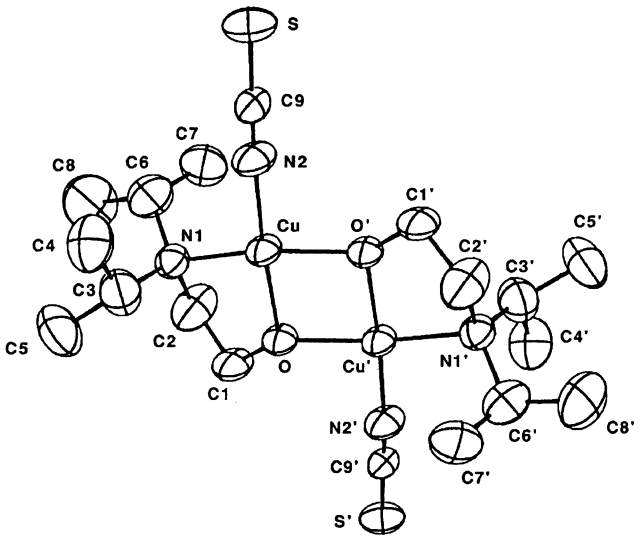

Fig. 1. ORTEP view of $[Cu_2(i\text{-}C_3H_7\text{-}L)_2(NCS)_2]$.

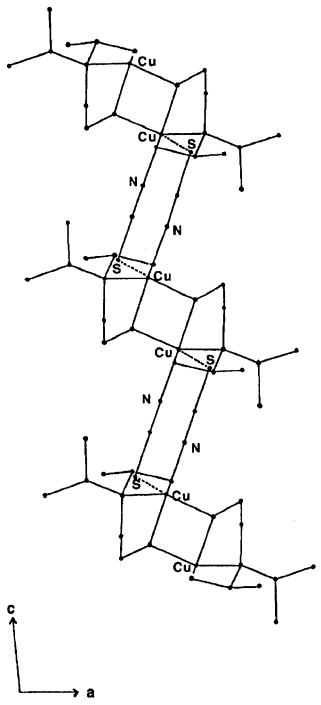

Fig. 2. Perspective view of chain structure of $[Cu_2(i\text{-}C_3H_7\text{-}L)_2(NCS)_2]$.

$[Cu_2(CH_3\text{-}L')_2(NCS)_2]$. As shown in Fig. 3, the complex consists essentially of dialkoxo-bridged centrosymmetric dinuclear units. The Cu···Cu′ distance is 2.988(1) Å and the Cu–O–Cu′ angle is 101.3(3)°. The geometry around the copper atom is an elongated square-pyramidal (4+1) environment. The two alkoxo oxygen atoms, an amino nitrogen atom, and a thiocyanato nitrogen atom form the basal plane with Cu giving bonds of 1.914(6), 1.950(5), 2.050(7), and 1.931(8) Å, respectively, which are typical for coordination bonds of dialkoxo-bridged dinuclear copper(II) complexes.[22—25] The apical site is occupied by the thiocyanate S atom of the neighboring molecule with a long bond to the copper ion (Cu···S 2.765(3) Å, Cu···Cu (interdimer) 5.537(1) Å). The dinuclear units are joined into a one-dimensional polymeric chain in the direction of the a-axis by thiocyanate bridges (Fig. 4).

$[Cu_2(C_2H_5\text{-}L')_2(NCS)_2]$. The crystal and molecular structure is similar to that of $[Cu_2(CH_3\text{-}L')_2(NCS)_2]$ (Figs. 5 and 6). The structure consists of $[Cu_2(C_2H_5\text{-}L')_2(NCS)_2]$ units which are further bridged by thiocyanate groups to yield a one-dimensional chain

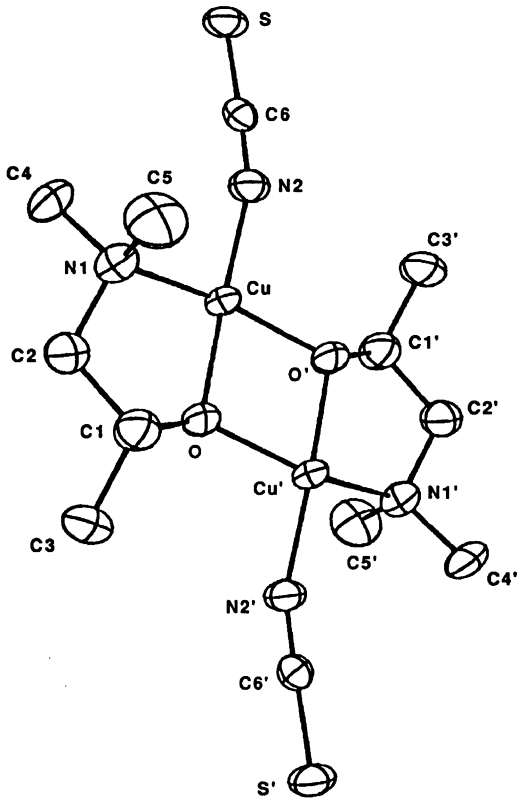

Fig. 3. ORTEP view of $[Cu_2(CH_3\text{-}L')_2(NCS)_2]$.

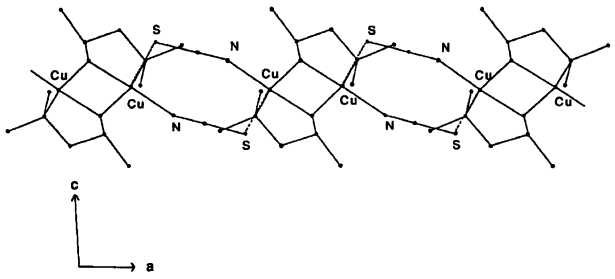

Fig. 4. Perspective view of chain structure of $[Cu_2(CH_3\text{-}L')_2(NCS)_2]$.

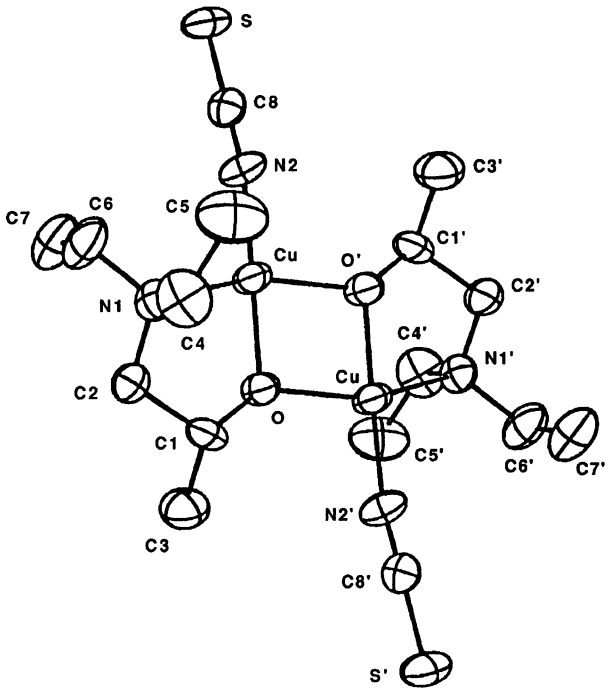

Fig. 5. ORTEP view of $[Cu_2(C_2H_5\text{-}L')_2(NCS)_2]$.

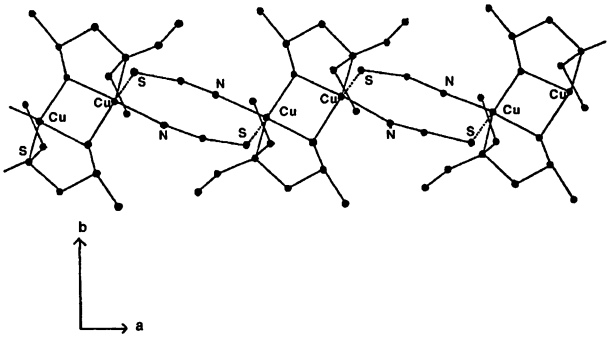

Fig. 6. Perspective view of chain structure of $[Cu_2(C_2H_5\text{-}L')_2(NCS)_2]$.

as shown in Fig. 6. The Cu···Cu′ separation is 2.975(1) Å and the Cu–O–Cu′ angle is 100.4(3)°. The Cu···S separation is 2.943(3) Å and the interdimer Cu···Cu separation is 5.805(2) Å.

$[Cu_2(n\text{-}C_3H_7\text{-}L')_2(NCS)_2]$. The crystal and molecular structure is similar to that of $[Cu_2(CH_3\text{-}L')_2(NCS)_2]$ (Figs. 7 and 8). The carbon atoms C7 and C8 of the propyl group showed some disorder. These have been modelled and the occupancies refined to 50:50 for positions C7a and C7b (C8a and C8b). The Cu···Cu′ separation is 2.981(1) Å and the Cu–O–Cu′ angle is 100.5(3)°. The Cu···S separation is 3.025(3) Å and the interdimer Cu···Cu separation is 5.887(1) Å.

$[Cu_2(i\text{-}C_3H_7\text{-}L')_2(NCS)_2]$. The molecular structure of $[Cu_2(i\text{-}C_3H_7\text{-}L')_2(NCS)_2]$ is illustrated in Fig. 9. The Cu···Cu′ distance is 2.963(1) Å and the Cu–O–Cu′ angle is 101.5(2)°. The coordination geometry around the copper atom is square-planar. The square plane around the copper atom is formed by two alkoxo oxygen atoms, an amino nitrogen atom, and a thiocyanate nitrogen atom. The Cu–O bond lengths (1.894(4) and 1.931(4) Å) and the Cu–N bond lengths (2.047(5) and 1.916(6) Å) fall in the range of those of the other alkoxo-bridged dinuclear copper(II) complexes.[22—25] The X-ray structure analysis of this compound does not reveal any close contacts between dinuclear units that may be regarded as bonding interaction (Fig. 10). The closest Cu···S contact between dinuclear units is 6.026(2) Å. This distance is substantially longer than the sum of the van der Waals radii of the copper and sulfur atoms. Thus, the crystal structure consists of discrete alkoxo-bridged dinuclear molecules.

Electronic Spectra. The present complexes show similar electronic spectra. The high-energy region of the spectra is characterized by the occurrence

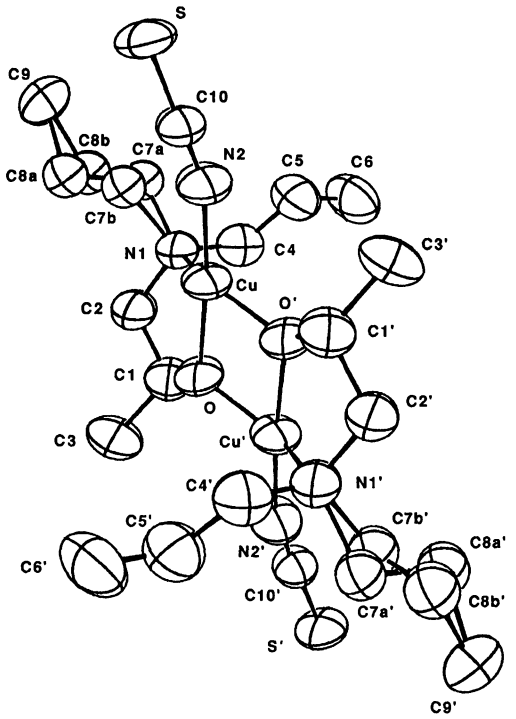

Fig. 7. ORTEP view of $[Cu_2(n\text{-}C_3H_7\text{-}L')_2(NCS)_2]$.

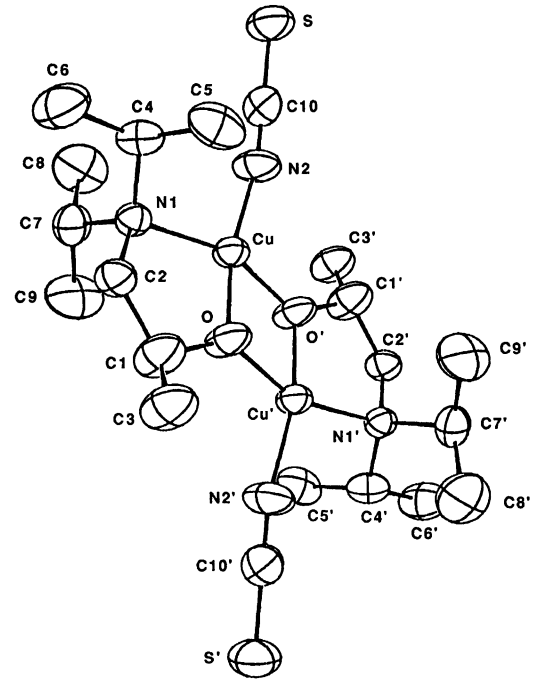

Fig. 9. ORTEP view of $[Cu_2(i\text{-}C_3H_7\text{-}L')_2(NCS)_2]$.

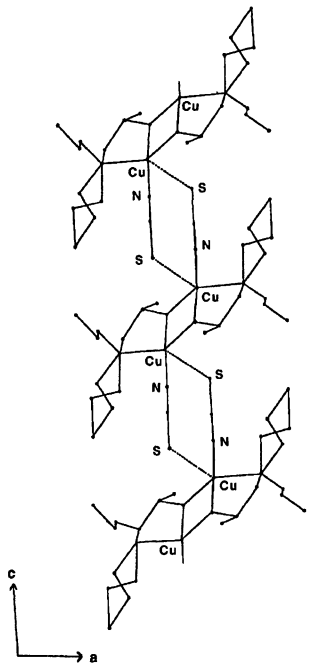

Fig. 8. Perspective view of chain structure of $[Cu_2(n\text{-}C_3H_7\text{-}L')_2(NCS)_2]$.

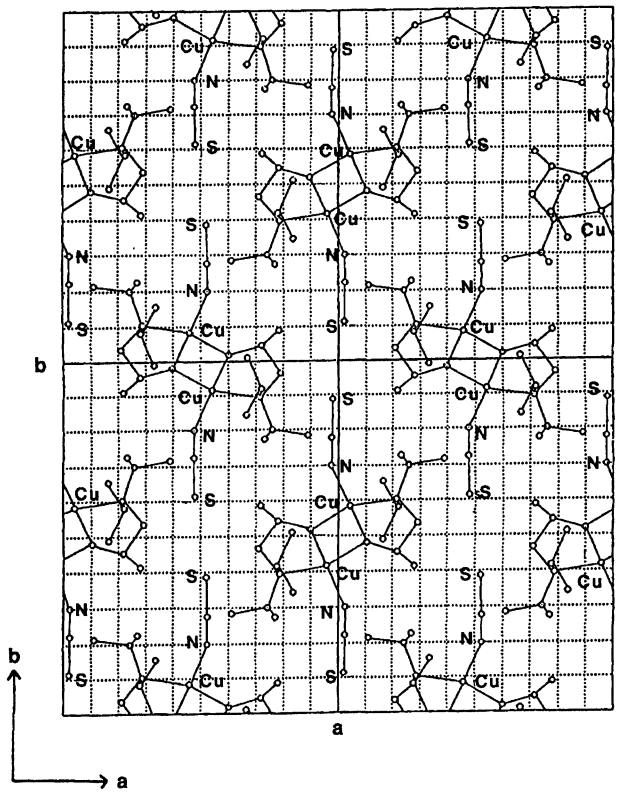

Fig. 10. Drawing of the structure viewed along c of $[Cu_2(i\text{-}C_3H_7\text{-}L')_2(NCS)_2]$.

of an intense band around 380 nm, which may be assigned to an alkoxo oxygen→copper(II) charge transfer transition.[16,24—26] The axial coordination effect of the thiocyanate-bridge can be observed in the d–d spectral region. As shown in Fig. 11, all the complexes except for $[Cu_2(i\text{-}C_3H_7\text{-}L')_2(NCS)_2]$ have a broad band with a tail around 900 nm which may correspond to the spectral pattern of five-coordinated square-pyramidal copper(II) complexes,[27] in contrast to the electronic spectrum of the discrete dinuclear complex, $[Cu_2(i\text{-}C_3H_7\text{-}L')_2(NCS)_2]$, which does not have any donor atom in the apical coordination site of the copper atom.

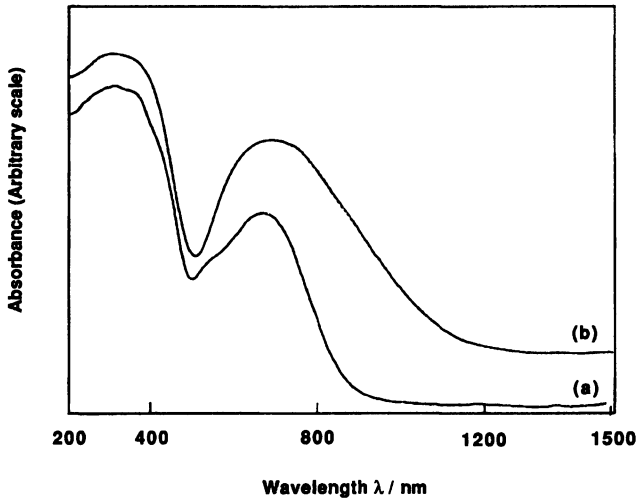

Fig. 11. Diffused reflectance spectra of $[Cu_2(i\text{-}C_3H_7\text{-}L')_2(NCS)_2]$ (a) and $[Cu_2(i\text{-}C_3H_7\text{-}L)_2(NCS)_2]$ (b).

Magnetic Susceptibilities. The effective magnetic moments of the present complexes fall in the range 1.26—1.56 B.M./Cu at room temperature, showing values lower than the expected spin-only magnetic moments. The temperature dependence of magnetic susceptibilities for all the complexes are shown in Figs. 12, 13, 14, 15, 16, 17, 18, and 19. The magnetic behaviors of $[Cu_2(CH_3\text{-}L)_2(NCS)_2]$ (Fig. 12) and $[Cu_2(C_2H_5\text{-}L)_2(NCS)_2]$ (Fig. 13) are similar to those of the previously reported ones.[16] The susceptibility data were fitted to the Bleaney–Bowers equation[6]

$$\chi_A = \frac{Ng^2\beta^2}{kT}[3+\exp(-2J/kT)]^{-1} + N\alpha, \qquad (1)$$

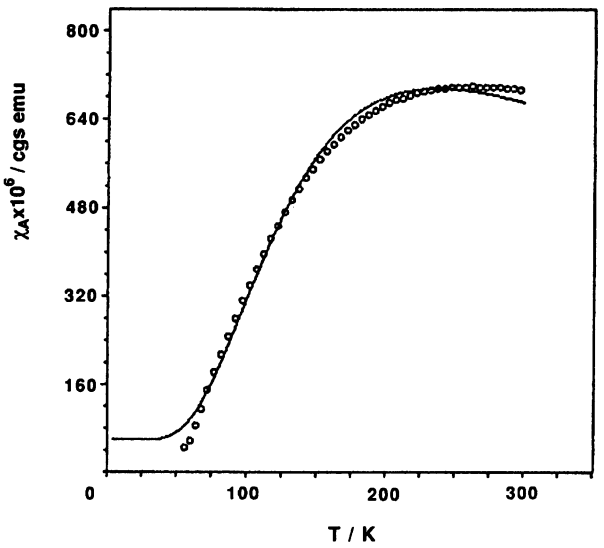

Fig. 12. Temperature dependence of the magnetic susceptibities of $[Cu_2(CH_3\text{-}L)_2(NCS)_2]$. The solid curve was calculated from the Bleaney–Bowers equation with $g=1.79$, $J=-132$ cm^{-1}, and $N\alpha=59\times10^{-6}$ cgs emu.

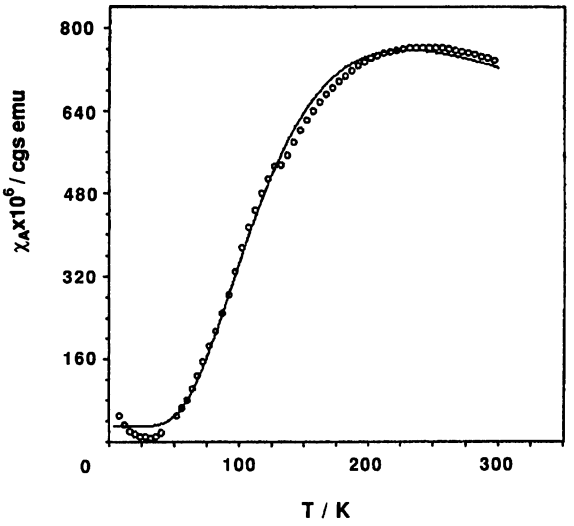

Fig. 13. Temperature dependence of the magnetic susceptibities of $[Cu_2(C_2H_5\text{-}L)_2(NCS)_2]$. The solid curve was calculated from the Bleaney–Bowers equation with $g=1.89$, $J=-128$ cm^{-1}, and $N\alpha=30\times10^{-6}$ cgs emu.

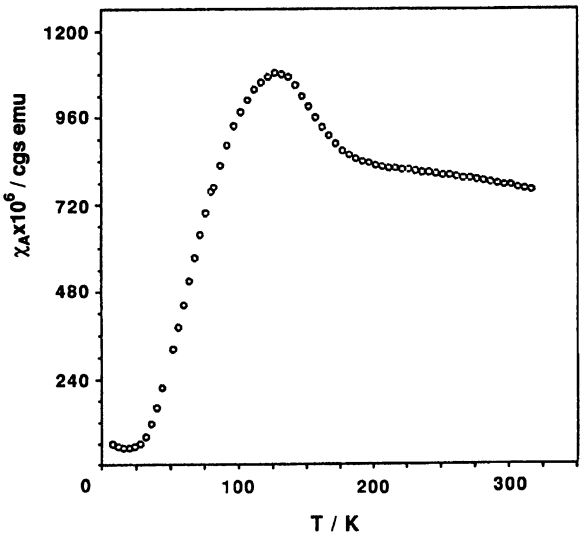

Fig. 14. Temperature dependence of the magnetic susceptibities of $[Cu_2(n\text{-}C_3H_7\text{-}L)_2(NCS)_2]$.

where $2J$ is the singlet-triplet energy gap defined by the Hamiltonian

$$\boldsymbol{H} = -2J\boldsymbol{S}_1\cdot\boldsymbol{S}_2, \qquad (2)$$

J expresses the intramolecular exchange interaction, S_1 and S_2 are quantum spin operators, and N, g, β, T, and $N\alpha$ have their usual meanings. Contrary to the previous failure in the fittings,[13,15—17] most of the present data can be fitted to the Bleaney–Bowers equation. In the case of $[Cu_2(CH_3\text{-}L')_2(NCS)_2]$, $[Cu_2(i\text{-}C_3H_7\text{-}L)_2(NCS)_2]$, and $[Cu_2(n\text{-}C_3H_7\text{-}L')_2(NCS)_2]$, the susceptibility data can be interpreted in terms of the Bleaney–Bowers equation with normal $2J$, g, and $N\alpha$ values (Figs. 16, 15, and 18). The $2J$ values (-330——-370 cm^{-1}) are comparable to those of the reported dialk-

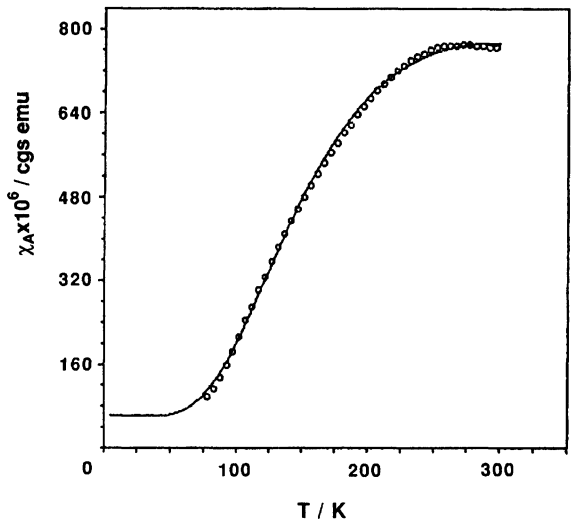

Fig. 15. Temperature dependence of the magnetic susceptibilities of $[Cu_2(i\text{-}C_3H_7\text{-}L)_2(NCS)_2]$. The solid curve was calculated from the Bleaney–Bowers equation with $g=2.12$, $J=-167$ cm^{-1}, and $N\alpha=61\times10^{-6}$ cgs emu.

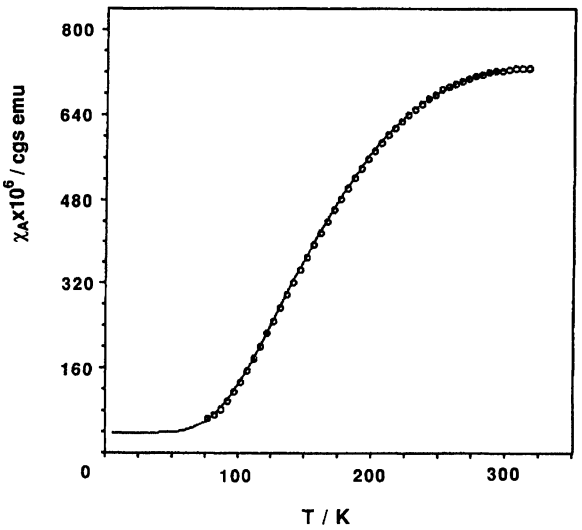

Fig. 16. Temperature dependence of the magnetic susceptibilities of $[Cu_2(CH_3\text{-}L')_2(NCS)_2]$. The solid curve was calculated from the Bleaney–Bowers equation with $g=2.21$, $J=-185$ cm^{-1}, and $N\alpha=38\times10^{-6}$ cgs emu.

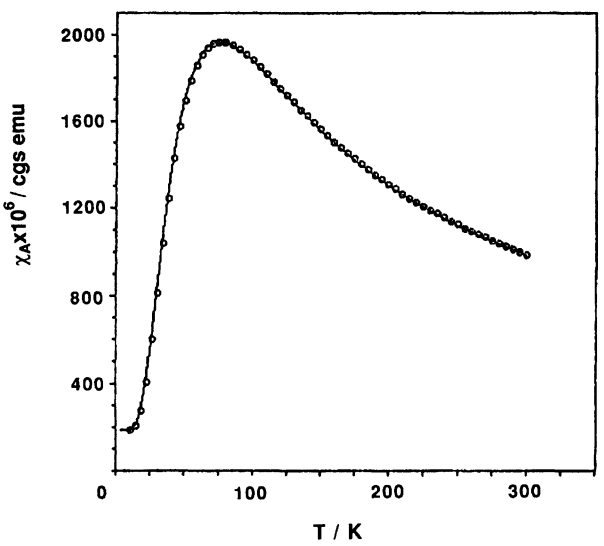

Fig. 17. Temperature dependence of the magnetic susceptibilities of $[Cu_2(C_2H_5\text{-}L')_2(NCS)_2]$. The solid curve was calculated from the Bleaney–Bowers equation with $g=1.70$, $J=-43$ cm^{-1}, and $N\alpha=186\times10^{-6}$ cgs emu.

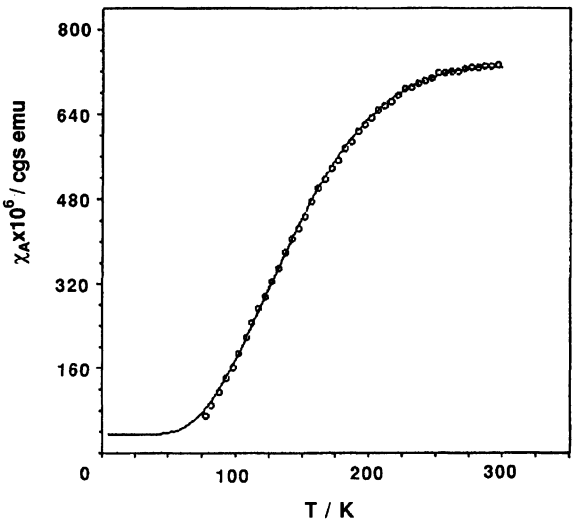

Fig. 18. Temperature dependence of the magnetic susceptibilities of $[Cu_2(n\text{-}C_3H_7\text{-}L')_2(NCS)_2]$. The solid curve was calculated from the Bleaney–Bowers equation with $g=2.09$, $J=-165$ cm^{-1}, and $N\alpha=35\times10^{-6}$ cgs emu.

oxo-bridged dinuclear copper(II) complexes, showing that a strong antiferromagnetic interaction is operating between the copper(II) ions.[24,25] On the other hand, attempts to fit the data for $[Cu_2(CH_3\text{-}L)_2(NCS)_2]$, $[Cu_2(C_2H_5\text{-}L)_2(NCS)_2]$, $[Cu_2(C_2H_5\text{-}L')_2(NCS)_2]$, and $[Cu_2(i\text{-}C_3H_7\text{-}L')_2(NCS)_2]$ to the Bleaney–Bowers equation gave unusual low g values ranging from 1.70 to 1.89 (Figs. 12, 13, 17, and 19), although their fits are good and show a fairly strong antiferromagnetic interaction ($2J=-86$——-264 cm^{-1}). This behavior may be the result of the polymeric chain structure of the present complexes, suggesting that interdimer interaction cannot be ruled out. From the structural data, a pathway for the interdimer magnetic interaction could be Cu⋯NCS⋯Cu / SCN unit. However, this pathway involves an axial position where the spin density is very low since in a distorted square-pyramidal geometry the unpaired electron is predominantly in a $d_{x^2-y^2}$ orbital (Chart 2). Because of this, a very slight overlap of the magnetic orbitals is expected for the interdimer coupling. Thus, it is difficult to attribute such an unusual magnetic behavior to the interdimer interaction.[28] In fact, the discrete din-

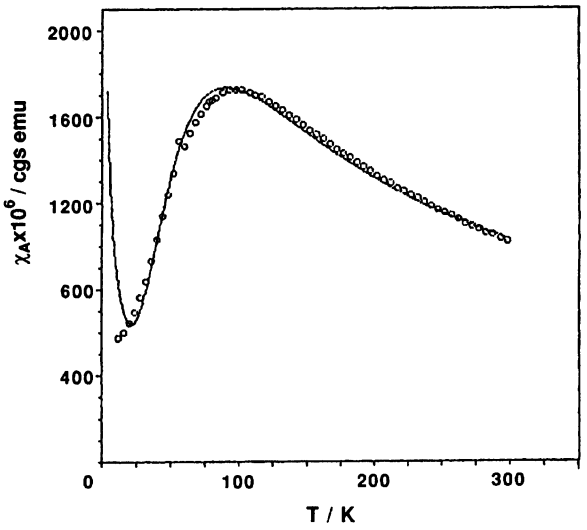

Fig. 19. Temperature dependence of the magnetic susceptibities of $[Cu_2(i\text{-}C_3H_7\text{-}L')_2(NCS)_2]$. The solid curve was calculated from the Bleaney–Bowers equation containing the paramagnetic impurity term,

$$\chi_A = \frac{(1-p)Ng^2\beta^2}{kT}[3+\exp(-2J/kT)]^{-1} + \frac{pNg^2\beta^2}{4kT} + N\alpha$$

with $g=1.70$, $J=-52$ cm^{-1}, and $N\alpha=256\times10^{-6}$ cgs emu, $p=0.027$. The fraction of paramagnetic impurity p was traeted as mononuclear Cu(II).

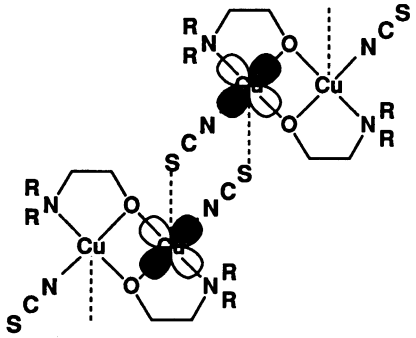

Chart 2.

uclear complex $[Cu_2(i\text{-}C_3H_7\text{-}L')_2(NCS)_2]$ shows a similar unusual magnetic behavior. As noted above, the X-ray analysis of $[Cu_2(i\text{-}C_3H_7\text{-}L')_2(NCS)_2]$ does not reveal any discernible exchange pathway between the dinuclear units. The complex would therefore be expected to act magnetically as an assemblage of dimers and to obey the Bleaney–Bowers equation. However, the best fit curve affords an unusually low g value, 1.70, to describe the susceptibility data (Fig. 19). As one of possible explanations, it may be assumed that some of the members of this series of complexes may have had their structures altered at low temperatures during the susceptibility measurements, resulting in the observed unusual magnetic behavior. There is an indication of a phase transition in the magnetic susceptibility data for $[Cu_2(C_2H_5\text{-}L)_2(NCS)_2]$ near 120 K (Fig. 13). In the case of $[Cu_2(n\text{-}C_3H_7\text{-}L)_2(NCS)_2]$, it was not possible to fit the complete data with use of the Bleaney–Bowers equation (Fig. 14). The χ_A vs. T curve for this complex exhibits a prominent maximum at 127 K. This maximum may be the outcome of a structural phase-transition. Such a phase-change behavior has already been observed in some dialkoxo-bridged dinuclear copper(II) complexes.[7—11]

Further investigations are still required in order to conclude about the origin of the unusual magnetic properties. Low-temperature X-ray crystallographic studies as well as differential scanning calorimetric analyses on these systems are in progress.

References

1) M. Kato, H. B. Jonassen, and J. C. Fanning, *Chem. Rev.*, **64**, 99 (1964).
2) A. P. Ginsberg, *Inorg. Chim. Acta, Rev.*, **5**, 45 (1971).
3) P. J. Hay, J. C. Thibeault, and R. Hoffmann, *J. Am. Chem. Soc.*, **97**, 4884 (1975).
4) A. Bencini and D. Gatteschi, *Inorg. Chim. Acta*, **31**, 11 (1978).
5) O. Kahn, *Angew. Chem., Int. Ed. Engl.*, **24**, 834 (1985).
6) B. Bleaney and K. D. Bowers, *Proc. R. Soc. London, Ser. A*, **214**, 451 (1952).
7) M. Mikuriya, H. Okawa, and S. Kida, *Bull. Chem. Soc. Jpn.*, **53**, 2871 (1980).
8) M. Mikuriya, H. Okawa, and S. Kida, *Bull. Chem. Soc. Jpn.*, **55**, 1086 (1982).
9) M. Mikuriya, K. Toriumi, T. Ito, and S. Kida, *Inorg. Chem.*, **24**, 629 (1985).
10) M. Mikuriya, H. Okawa, and S. Kida, *Bull. Chem. Soc. Jpn.*, **54**, 2979 (1981).
11) M. Mikuriya and K. Toriumi, *Bull. Chem. Soc. Jpn.*, **66**, 2106 (1993).
12) O. Kahn, I. M. -Badarau, J. P. Audiere, J. M. Lehn, and S. A. Sullivan, *J. Am. Chem. Soc.*, **102**, 5936 (1980).
13) M. Lehtonen, E. Luukkonen, and R. Uggla, *Suom. Kemistil. B*, **44**, 399 (1971).
14) A. Pajunen and K. Smolander, *Finn. Chem. Lett.*, **1974**, 99.
15) W. Haase, R. Mergehenn, and W. Krell, *Z. Naturforsch., B*, **31b**, 85 (1976).
16) Y. Nishida and S. Kida, *J. Inorg. Nucl. Chem.*, **38**, 451 (1976).
17) M. Mikuriya, Y. Nishida, S. Kida, T. Uechi, and I. Ueda, *Acta Crystallogr., Sect. B*, **33**, 538 (1977).
18) W. W. Hartman, *Org. Synth.*, **2**, 183 (1943).
19) A. R. Goldfarb, *J. Am. Chem. Soc.*, **63**, 2280 (1941).
20) P. W. Selwood, "Magnetochemistry," Interscience Publishers, New York (1956), pp. 78 and 91.
21) B. A. Frenz, "The SDP-User's Guide, " Enraf-Nonius, Delft, The Netherlands (1985).
22) A. C. Villa, L. Coghi, A. G. Manfredotti, and C. Guastini, *Cryst. Struct. Commun.*, **3**, 543 (1974).
23) N. Matsumoto, S. Kida, and I. Ueda, *J. Coord. Chem.*, **9**, 133 (1979).

24) M. Handa, T. Idehara, K. Nakao, K. Kasuga, M. Mikuriya, N. Matsumoto, M. Kodera, and S. Kida, *Bull. Chem. Soc. Jpn.*, **65**, 3241 (1992), and references therein.
25) M. Mikuriya, *Trends Inorg. Chem.*, **2**, 131 (1991), and references therein.
26) S. Kida, Y. Nishida, and M. Sakamoto, *Bull. Chem. Soc. Jpn.*, **46**, 2428 (1973).
27) A. B. P. Lever, "Inorganic Electronic Spectroscopy," Elsevier, Amsterdam (1984), pp. 554—611.
28) Preliminary analyses based on an alternating chain model could not fit the magnetic data by using normal g values and gave similar results to those of the Bleaney–Bowers dimer model.